

## A STABLE MULTIGRID STRATEGY FOR CONVECTION-DIFFUSION USING HIGH ORDER COMPACT DISCRETIZATION\*

ANAND L. PARDHANANI<sup>†</sup>, WILLIAM F. SPOTZ<sup>‡</sup>, AND GRAHAM F. CAREY<sup>§</sup>

**Abstract.** Multigrid schemes based on high order compact discretization are developed for convection-diffusion problems. These multigrid schemes circumvent numerical oscillations and instability, while also yielding higher accuracy. These instabilities are typically exacerbated by the coarser grids in multigrid calculations. Our approach incorporates a 4th order compact formulation for the discretization, while also constructing a consistent multigrid restriction scheme to preserve the accuracy of the fine-to-coarse grid projections. Numerical results demonstrating the higher accuracy and robustness of this approach are presented for representative 2D convection-diffusion problems. These calculations also confirm that our numerical algorithms exhibit the typical multigrid efficiency and mesh-independent convergence properties.

**Key words.** convection-diffusion, high-order compact discretizations, multigrid.

**AMS subject classifications.** 65F10,65N06,65N22,65N55.

**1. Introduction.** Convection-diffusion problems in which convective effects are strong frequently exhibit steep boundary layers or interior layers within the domain. When conventional methods are used to solve such problems, the cell Peclet (or Reynolds) number imposes restrictions on the permissible mesh size – the solution is oscillatory when the mesh is too coarse. The usual techniques for circumventing this problem in standard single-grid formulations include the use of artificial dissipation, upwind discretizations, mesh grading and/or refinement [1, 3].

When multigrid methods are used for solving convection-diffusion problems, these difficulties are exacerbated [2]. The use of coarser grid levels introduces a new source of problems since, even if the finest grid satisfies the mesh restrictions, one or more coarser grids may violate it. Various techniques for dealing with such problems have been proposed in recent years [2, 8, 9, 14]. Some of these are based on extensions of the standard single-grid techniques, while certain others are designed specifically for use with multigrid methods. The degree of effectiveness varies with choice of technique, and each of them has limitations in terms of efficiency and robustness. In the present work we develop a multigrid strategy based on high-order compact (HOC) discretizations that yields higher accuracy and robustness when applied to convection-diffusion problems. This is conceptually similar to the strategy used by Gupta et al. [5, 6], but differs in the formulation of the discretization scheme and the multigrid projections between different grid levels, as discussed in Section 2. There we present the model 2D convection-diffusion problem and its higher-order compact approximation, and we also describe the associated multilevel projections for the HOC scheme. In Section 3 we show results for three specific test problems, and compare the HOC multigrid calculations with more standard schemes to demonstrate its numerical behavior.

**2. Model Problem and HOC Scheme.** For simplicity of exposition we consider the familiar steady convection-diffusion model PDE

$$(2.1) \quad -\Delta u + \alpha \cdot \nabla u = f$$

\* Received June 10, 1997. Accepted August 27, 1997. Communicated by J. Pasciak. This research was supported in part by DARPA contract # DABT 63-92-C-0024.

<sup>†</sup> CFD Laboratory, The University of Texas, Austin, Texas 78712. (anand@cfdlab.ae.utexas.edu)

<sup>‡</sup> NCAR, P.O. Box 3000, Boulder, Colorado 80307. (spotz@ucar.edu)

<sup>§</sup> CFD Laboratory, The University of Texas, Austin, Texas 78712. (carey@cfdlab.ae.utexas.edu)

where  $\alpha = (c, d)$  and  $f$  may all be functions of  $(x, y)$  in general. A variety of test cases can be constructed from this framework for given convective velocity  $\alpha$  by choosing the form of the solution  $u$  and determining a corresponding source function  $f$ .

The idea of operating on the differential equation as an auxiliary relation to obtain expressions for higher-order derivatives in the truncation error has been exploited in, for instance, defect-correction schemes and also the classical Lax-Wendroff method to yield a stable scheme for differencing hyperbolic problems. Recently we have generalized and expanded upon these concepts to develop a class of difference methods that exhibit higher-order asymptotic accuracy, while still using only a simple stencil of nodes surrounding a grid point. We refer to these schemes as high-order compact (HOC) methods (e.g., see [11, 12]). Inclusion of these approximations in a central difference method for (2.1) increases the order of accuracy, typically to  $O(h^4)$  while still retaining the compact stencil defined by a grid point and its immediate neighbors. In addition to the higher accuracy, which allows problems to be solved on coarser grids, HOC schemes have been shown to suppress oscillations in transport simulations [10, 11]. This behavior suggests that they might work well in conjunction with multigrid strategies for convection-diffusion applications.

For clarity of exposition let us introduce the HOC formulation by first considering the 1D form of (2.1)

$$(2.2) \quad -u'' + cu' = f$$

Introducing a uniform grid  $x_i$  with spacing  $h$  and central differencing, the representative difference equation at interior node  $i$  is simply

$$(2.3) \quad -\delta_x^2 u_i + c_i \delta_x u_i = f_i$$

where  $\delta_x$  and  $\delta_x^2$  denote the first and second order central difference approximations on a uniform mesh with spacing  $h$ . The associated truncation error is

$$(2.4) \quad \tau_i = \frac{h^2}{12}(2c_i u_i''' - u_i^{iv}) + O(h^4)$$

As is well known, the scheme (2.3) yields oscillatory solutions if the cell Peclet condition  $ch < 2$  is violated. It can also be easily verified that in a multigrid solution of (2.3), even if the fine grid satisfies the cell condition, the overall scheme may diverge if coarser levels violate the condition.

A HOC scheme can be constructed by differentiating the transport equation to obtain expressions for  $u'''$  and  $u^{iv}$  and then substituting in (2.4) to obtain, after central difference, the HOC formula

$$(2.5) \quad -A_i \delta_x^2 u_i + C_i \delta_x u_i = F_i$$

with

$$\begin{aligned} A_i &= 1 + \frac{h^2}{12}(c_i^2 - 2\delta_x c_i), \\ C_i &= c_i + \frac{h^2}{12}(\delta_x^2 c_i - c_i \delta_x c_i), \\ F_i &= f_i + \frac{h^2}{12}(\delta_x^2 f_i - c_i \delta_x f_i) \end{aligned}$$

We emphasize that  $F_i$  is obtained by applying an HOC operator to the nodal values  $f_i$ . This will influence the construction of inter-grid transfer operators in the multigrid scheme, as we

will see later. The resulting scheme has been demonstrated to be nonoscillatory for the standard model 1D convection-diffusion test problem, independent of mesh-size  $h$  [10, 11]. This suggests that multigrid schemes with discretization and projections based on HOC representations may not be prone to the divergence problems mentioned previously.

We next present the HOC scheme for the 2D problem (2.1) and discuss the associated multigrid implementation. The basic derivation proceeds as in the 1D case above and hence we will simply sketch the construction and give the final form of the discrete HOC scheme. We assume a uniform mesh (extension of the HOC approach to nonuniform grids and mapping is discussed elsewhere [13]). Central differencing (2.1) we obtain

$$(2.6) \quad -(\delta_x^2 + \delta_y^2)u_{ij} + (c_{ij}, d_{ij}) \cdot (\delta_x, \delta_y)u_{ij} = f_{ij}$$

The truncation error for (2.6) is

$$(2.7) \quad \tau_{ij} = \frac{h^2}{12} \left[ 2 \left( c \frac{\partial^3 u}{\partial x^3} + d \frac{\partial^3 u}{\partial y^3} \right) - \left( \frac{\partial^4 u}{\partial x^4} + \frac{\partial^4 u}{\partial y^4} \right) \right]_{ij} + O(h^4).$$

As in the 1D case, expressions for the higher derivatives in the truncation error can be obtained by differentiating the PDE. After substituting the corresponding expressions in (2.7) and central differencing we obtain the following HOC approximation for (2.1)

$$(2.8) \quad \begin{aligned} & -A_{ij}\delta_x^2 u_{ij} - B_{ij}\delta_y^2 u_{ij} + C_{ij}\delta_x u_{ij} + D_{ij}\delta_y u_{ij} - \\ & \frac{h^2}{6} [\delta_x^2 \delta_y^2 u_{ij} - c_{ij}\delta_x \delta_y^2 u_{ij} - d_{ij}\delta_x^2 \delta_y u_{ij} - G_{ij}\delta_x \delta_y u_{ij}] = \\ & F_{ij} + O(h^4), \end{aligned}$$

where the coefficients  $A_{ij}$ ,  $B_{ij}$ ,  $C_{ij}$ ,  $D_{ij}$ ,  $F_{ij}$  and  $G_{ij}$  are given by

$$\begin{aligned} A_{ij} &= 1 + \frac{h^2}{12} (c_{ij}^2 - 2\delta_x c_{ij}), \\ B_{ij} &= 1 + \frac{h^2}{12} (d_{ij}^2 - 2\delta_y d_{ij}), \\ C_{ij} &= c_{ij} + \frac{h^2}{12} (\delta_x^2 c_{ij} + \delta_y^2 c_{ij} - c_{ij}\delta_x c_{ij} - d_{ij}\delta_y c_{ij}), \\ D_{ij} &= d_{ij} + \frac{h^2}{12} (\delta_x^2 d_{ij} + \delta_y^2 d_{ij} - c_{ij}\delta_x d_{ij} - d_{ij}\delta_y d_{ij}), \\ F_{ij} &= f_{ij} + \frac{h^2}{12} (\delta_x^2 f_{ij} + \delta_y^2 f_{ij} - c_{ij}\delta_x f_{ij} - d_{ij}\delta_y f_{ij}), \\ G_{ij} &= \delta_y c_{ij} + \delta_x d_{ij} - c_{ij}d_{ij}. \end{aligned}$$

For convenience in our later analyses, we replace the  $i, j$ -index with a single global index for the nodes, and rewrite equation (2.8) in matrix-vector notation as

$$(2.9) \quad \sum_l M_{kl} u_l = F_k + O(h^4)$$

where,  $k$  and  $l$  denote the standard matrix indexing system, and (2.9) applies at any interior node  $(x_k, y_k)$ . Introducing the superscript notation to denote mesh spacing for multigrid analysis, and assembling (2.9) over the whole mesh, we get a matrix system of the form

$$(2.10) \quad \mathbf{M}^h \mathbf{u}^h = \mathbf{F}^h$$

Implementing the HOC formulation within a multigrid framework involves modifying the usual procedure for constructing the matrix on the fine and coarse grids to include computing derivatives of the PDE coefficients and allowing for a 9-point stencil. In addition, the restriction procedure and the right hand side of the matrix systems must be modified if 4th order consistency of the algorithm is to be enforced at all grid levels.

To illustrate the modified procedure for fine-to-coarse restriction of residuals, consider the original PDE rewritten in operator form

$$(2.11) \quad Lu = f$$

where

$$(2.12) \quad L \equiv -\Delta + \boldsymbol{\alpha} \cdot \nabla$$

Let  $u^*$  denote a smooth interpolant of the fine grid approximation  $u_h^*$ . Then we can write (2.11) as

$$(2.13) \quad 0 = L(u - u^* + u^*) - f = L(e^*) + L(u^*) - f = L(e^*) - r$$

where  $r = f - L(u^*)$ . The HOC approximation of  $Le^* = r$  on the fine grid  $\Omega_h$  follows from

$$(2.14) \quad 0 = (Le^* - r)|_{x_k} = \sum_l M_{kl} e_l^* - \hat{r}_k - \tau_k$$

as

$$(2.15) \quad M^h e^{h*} = \hat{r}^h, \quad \hat{r}^h = \hat{f}^h - (\widehat{Lu^*})^h$$

We use the “hat” notation to denote quantities evaluated by applying an HOC difference formula to their nodal values. This is to distinguish them from similar quantities that are evaluated directly at the nodes, which are written without the “hat” notation. Similarly, the HOC approximation on the coarse grid  $\Omega_H$  is

$$(2.16) \quad M^H e^{H*} = \hat{r}^H, \quad \hat{r}^H = \hat{f}^H - (\widehat{Lu^*})^H$$

Using the linearity of  $L$  and the fact that the residual is evaluated at the nodes, it follows that  $\hat{r}^H$  can be obtained directly from  $\hat{r}^h$  and this is constructed precisely as in (2.8) using the nodal values  $r_k$ . For example, in the 1D case described in (2.5) we have

$$(2.17) \quad \hat{r}_k^H = \frac{H^2}{12} (\delta_x^2 r_k - c_k \delta_x r_k)$$

at the coarse grid nodes  $k$ , where  $\delta_x^2, \delta_x$  are the coarse grid difference operators. Note that this also implies that the residuals at the additional (non-nested) nodes on the fine grid need not be evaluated. However, in practice we simply compute  $r^h = \hat{f}^h - M_h u^{h*}$  on the fine grid and then use it in (2.17) to compute  $\hat{r}^H$  at the coarser grid nodes. Finally, the solution of (2.16) gives the coarse grid correction  $e^{H*}$ , and this can be added directly componentwise to the fine grid approximation  $u^{h*}$ .

Let  $P$  denote the  $m \times n$  restriction matrix for the map from fine to coarse grid. Then the restriction operation can be written as

$$(2.18) \quad r^H = P r^h$$

where  $P$  has the necessary unit entries in the appropriate row and column locations to “extract” the coarse grid vector and zero entries elsewhere. The right side vector for the HOC scheme then follows from (2.17) where the entries  $r_i$  correspond to  $r^H$  in (2.18). The corresponding prolongation operator is  $P^T$  and we have the fine grid update

$$(2.19) \quad e^h = P^T e^{H^*}$$

where  $e^{H^*}$  is obtained by solving the coarse grid system (2.16).

**Remark:** Note that in this approach we use the continuous differential problem  $Lu = f$  in  $\Omega$  to construct the coarse grid problem and deduce the corresponding restriction and prolongation operators. In so doing we pose consistent  $O(h^4)$  and  $O(H^4)$  HOC schemes at the respective levels. Keeping in mind that the main purpose of the multigrid scheme is, however, to act as a preconditioning to the fine grid problem, the need for a high-order scheme for the coarse grid problem is moot. Instead, the gain may lie in the fact that the  $O(H^4)$  scheme should have better oscillatory stability properties and avoid the need for adding artificial dissipation or using other heuristic approaches for the coarse grid problem (e.g., see Gupta et al. [5, 6]). In fact, for the 1D case the HOC scheme is nonoscillatory for the model convection-diffusion problem at all Reynolds (Peclet) numbers, which suggests this idea has some merit.

In the next section we show the results of numerical studies in 2D that are designed to test the method. We also emphasize that the preferred approach for constructing the coarse grid problem may not necessarily be through the approximation of the PDE on this grid. Instead it might be preferable to construct the Schur complement problem for the coarse grid and then approximate this problem to determine a convenient class of coarse grid discrete systems with associated restriction and prolongation operators. We will explore this topic and related issues in a subsequent study.

**3. Results and Discussion.** Numerical studies using our approach have been carried out for the convection-diffusion equation (2.1) subject to Dirichlet boundary conditions. We consider both constant and variable coefficients in our test problems, which are listed below.

**Problem 1:**

The domain is  $0 < x, y < 1$ ,  $c = d = \text{constant}$ ,  $f = 0$ , and the analytical solution is

$$(3.1) \quad u(x, y) = [(e^{cx} - 1)/(e^c - 1)][(e^{dy} - 1)/(e^d - 1)]$$

For  $c$  and  $d$  large and positive, the solution has a corner layer near  $(1, 1)$ .

**Problem 2:**

The domain is  $-0.5 < x, y < 0.5$ ,  $c = d = \text{constant}$ ,  $f$  is derived by substituting the following analytical solution into (2.1)

$$(3.2) \quad u(x, y) = \tanh[q(x^2 + y^2 - r^2)]$$

with  $q = 10$  and  $r = 0.25$ . This solution has a steep layer along the circumference of a circle of radius 0.25 centered at the origin. The value of  $q$  controls the magnitude of the gradients.

**Problem 3:**

The domain is  $0 < x, y < 1$ , the coefficients have the form  $c = -Rx$  and  $d = Ry$ , the source term  $f$  is derived by substituting the following analytical solution into (2.1)

$$(3.3) \quad u(x, y) = xy(1 - x)(1 - y)e^{(x+y)}$$

Here  $R$  is a constant parameter whose magnitude determines the severity of convection domination in the problem. This is among the test problems used by Gupta et al. [7].

In the numerical studies we consider a range of convection to diffusion ratios, as well as the influence of mesh spacing and number of levels in the multigrid algorithm. The results show that the HOC approach improves multigrid stability, preserves the typical mesh-independent convergence behavior of the multigrid cycles and yields 4th order accuracy.

The results presented here are computed using multigrid  $V$ -cycles, with Gauss-Seidel relaxation for 2 pre-smoothing and 1 post-smoothing iteration. We have considered restriction based on full-weighting as well as the self-consistent HOC form discussed previously. Bilinear interpolation is used for coarse-to-fine projections, and a band solver is used at the coarsest level.

Figures 3.1-3.3 show convergence behavior of the residual as a function of multigrid cycles for each test problem for a range of convection to diffusion ratios. In each case we use a 6-level multigrid cycle starting from a  $65 \times 65$  fine grid. These figures demonstrate how the HOC formulation improves stability and permits the use of much higher convection to diffusion ratios for a given mesh size. If we use 2nd order central differencing in place of the HOC discretization, the multigrid cycles are far less stable – as the convection ratio increases, it limits the coarser mesh levels permissible for convergence. For example, with a convection to diffusion ratio of 50 – the least severe case in Figure 3.1 – multigrid convergence is not possible without limiting it to a 3-level cycle with  $17 \times 17$  nodes on the coarsest level. This leads to a considerable increase in the computational cost compared to the HOC case, where the coarsest mesh has  $3 \times 3$  nodes. Figure 3.4 compares the convergence behavior of the two schemes as a function of CPU time for this case. In fact, the CDS performance rapidly gets worse as the convection is increased further, until we get to the point where the finest grid itself is inadequate for computing a stable, nonoscillatory solution. Similar results are observed when the central difference scheme is used in Problems 2 and 3.

Figures 3.5-3.7 demonstrate the mesh-independent convergence behavior of the multigrid cycles for the HOC formulation. Each curve represents a multigrid calculation with the indicated fine mesh spacing, and  $V$ -cycles that descend all the way to the coarsest level that is nested within the finest mesh. Other details of the multigrid cycle are the same as those specified for the cases in the previous figures. The figures clearly show that the residual converges at a similar rate even as we refine the finest mesh.

Figures 3.8-3.10 show that the HOC formulation yields 4th order accuracy in the numerical solution. In each case, the RMS error in the numerical solution at the finest grid points (relative to the known analytical solution) is plotted as a function of finest mesh spacing. The slope of the straight line on the log-log plots is very close to 4 for each test problem.

As noted earlier, in convection-diffusion computations with 2nd order central schemes, converged numerical solutions at high Peclet or Reynolds numbers may exhibit spatial oscillations if the grid is not sufficiently fine [4]. In our test problems we confirm that the numerical results using the HOC approach are oscillation-free by inspecting surface plots of the solution. Figure 3.11 shows such a plot for Problem 2 with  $c = d = 500$  using a  $65 \times 65$  fine grid. This represents the most stringent case considered in Figure 3.2 where we see the rate of multigrid convergence starting to break down at this convection level. Figure 3.12 shows a similar plot for a  $33 \times 33$  fine grid with  $c = d = 200$ , which is the worst case in Figure 3.6.

Our numerical studies also revealed certain other interesting features of the HOC multigrid approach. For instance, when standard multigrid strategies are applied to convection-diffusion problems, stability is not guaranteed even when the finest mesh satisfies the usual

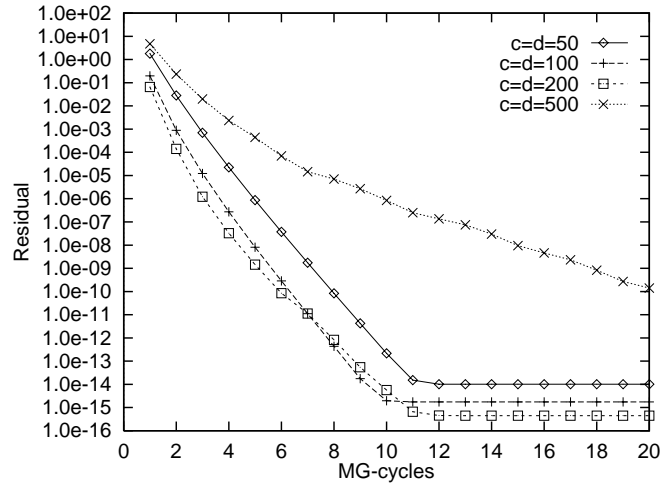


FIG. 3.1. Convergence behavior of HOC method for Problem 1 on a  $65 \times 65$  fine grid with a 6-level HOC-consistent multigrid cycle for various convection to diffusion ratios.

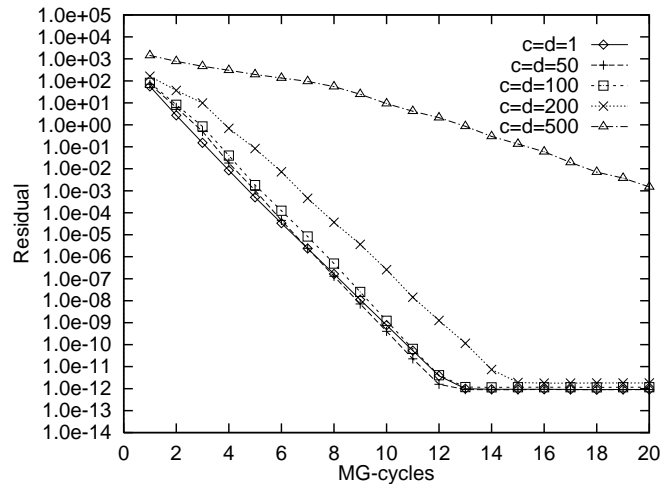


FIG. 3.2. Convergence behavior of HOC method for Problem 2 with similar multigrid cycle as that of Fig. 3.1.

Pecllet (or Reynolds) condition for stability. In the 2nd order central difference scheme with a given fine mesh, as the convection increases, the number of permissible coarser levels decreases. Otherwise the coarsest mesh levels contribute to instability of the multigrid algorithm. In contrast, with the HOC formulation multigrid stability seems less sensitive to the coarser levels. As long as the fine grid is adequate to yield stable solutions, the number and coarseness of the other levels appears irrelevant to the stability of the multigrid algorithm.

Finally, we also investigated the behavior of the HOC multigrid algorithm for very large Reynolds numbers. We found the method converged for the highest Reynolds numbers that we tested ( $c = d = 10^5$  in Problem 1). However, the convergence rate significantly deteriorates, as shown in Figure 3.13 which plots the residual as a function of multigrid cycles for Problem 1 with values of  $c$  and  $d$  much larger than in Figure 3.1. We emphasize that the

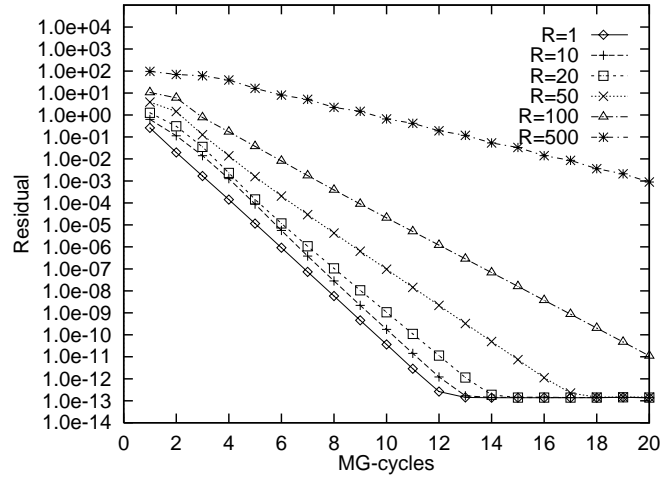


FIG. 3.3. Convergence behavior of HOC method for Problem 3 with similar multigrid cycle to that of Fig. 3.1.

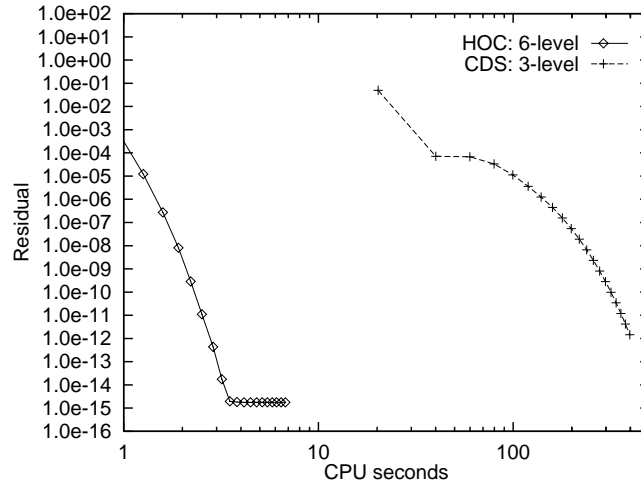


FIG. 3.4. CPU timing comparison of HOC and central difference (CDS) multigrid schemes for Problem 1 with convection to diffusion ratio of 50.

results in Figure 3.13 were computed with the same grid and multigrid cycling strategy as was used in Figure 3.1.

**4. Conclusion.** We have developed an accurate, robust multigrid approach for convection-diffusion applications using high order compact finite difference discretizations. The resulting numerical scheme preserves the stability and mesh-independent convergence properties of the multigrid computations, while also yielding a 4th order accurate, non-oscillatory solution at the finest mesh level. The high order compact formulation is used for discretizing the problem at all grid levels, as well as for constructing consistent multigrid projections from fine to coarse grids. Our numerical studies on 2D convection-diffusion problems demonstrate the stability and accuracy of this approach in the multigrid setting. Compared to the standard 2nd order central differencing strategy, the HOC method yields significantly higher stability, accuracy and computational efficiency. It permits the use of the full hierarchy of nested

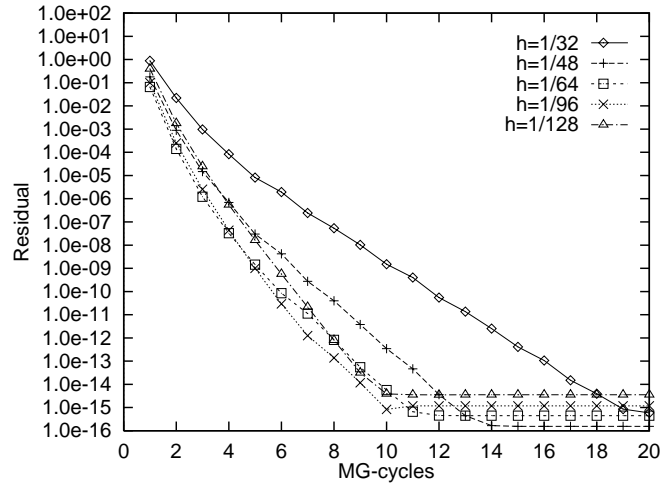


FIG. 3.5. Mesh-independent convergence behavior of HOC-consistent multigrid cycles for Problem 1 with  $c = d = 200$ .

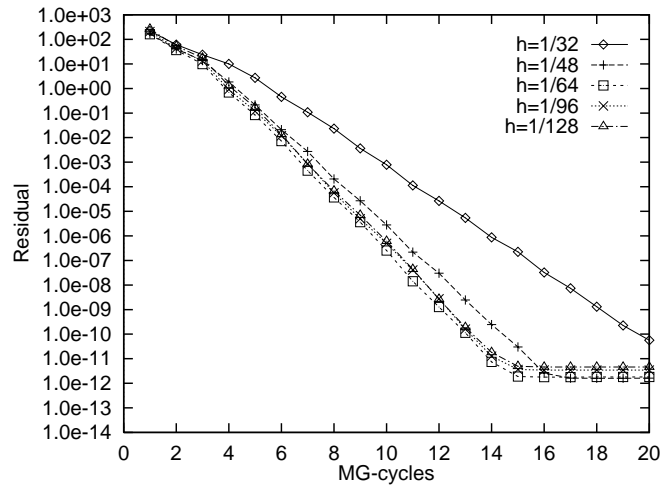


FIG. 3.6. Mesh-independent convergence behavior of HOC-consistent multigrid cycles for Problem 2 with  $c = d = 200$ .

coarse grids in the multigrid algorithm, unlike the central difference approach which limits the number of coarse meshes depending on the convection to diffusion ratio.

#### REFERENCES

- [1] G. F. CAREY AND J. T. ODEN, *Finite Elements: Computational Aspects*, Prentice-Hall, Englewood Cliffs, N.J., 1984.
- [2] G. F. CAREY AND A. PARDHANANI, *Multigrid solution and grid redistribution for convection-diffusion*, *Internat. J. Numer. Methods Engrg.*, 27(1989), pp. 655–664.
- [3] G. F. CAREY AND T. PLOVER, *Variable upwinding and adaptive mesh refinement in convection-diffusion*, *Internat. J. Numer. Methods Engrg.*, 19(1983), pp. 341–353.

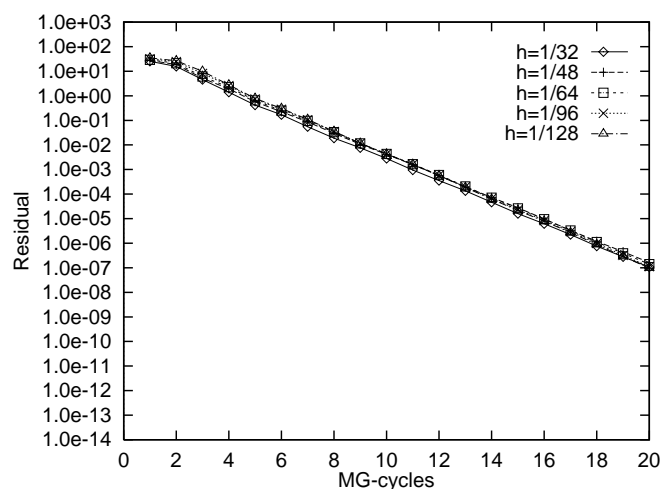


FIG. 3.7. Mesh-independent convergence behavior of HOC-consistent multigrid cycles for Problem 3 with  $R = 200$ .

[4] P. M. GRESHO AND R. L. LEE, *Don't suppress the wiggles – they're telling you something!*, *Comput. & Fluids*, 9(1981), pp. 223–253.

[5] M. M. GUPTA, J. KOUATCHOU, AND J. ZHANG, *A compact multigrid solver for convection-diffusion equations*, *J. Comput. Phys.*, to appear.

[6] ———, *Comparison of 2nd and 4th order discretizations for multigrid poisson solvers*, *J. Comput. Phys.*, to appear.

[7] M. M. GUPTA, R. P. MANOHAR, AND J. W. STEPHENSON, *A single cell high order scheme for the convection-diffusion equation with variable coefficients*, *Internat. J. Numer. Methods Fluids*, 4(1984), pp. 641–651.

[8] W. HACKBUSCH, *Multi-Grid Methods and Applications*, Springer Series in Computational Mathematics, volume 4, Springer-Verlag, Berlin, 1985.

[9] P. W. HEMKER, *Mixed defect correction iteration for the accurate solution of the convection diffusion equation*, In *Multigrid Methods: Proceedings of conference held in Köln-Porz, November 23-27, 1981*, W. Hackbusch and U. Trottenberg, eds., volume 960 of *Lecture Notes in Mathematics*, Springer-Verlag, Berlin, 1982, pp. 492–503.

[10] R. J. MACKINNON AND R. W. JOHNSON, *Differential equation based representation of truncation errors for accurate numerical simulation*, *Internat. J. Numer. Methods Fluids*, 13(1991), pp. 739–757.

[11] W. F. SPOTZ AND G. F. CAREY, *High-order compact scheme for the stream-function vorticity equations*, *Internat. J. Numer. Methods Engrg.*, 38(1995), pp. 3497–3512.

[12] ———, *A high-order compact formulation for the 3D Poisson equation*, *Numer. Methods Partial Differential Equations*, 12(1996), pp. 235–243.

[13] ———, *Formulation and experiments with high-order compact schemes for nonuniform grids*, *Internat. J. Numer. Methods Heat Fluid Flow*, Submitted May, 1996.

[14] P. M. De Zeeuw and E. J. Van Asselt, *The convergence rate of multi-level algorithms applied to the convection-diffusion equation*, *SIAM J. Sci. Statist. Comput.*, 6(1985), pp. 492–503.

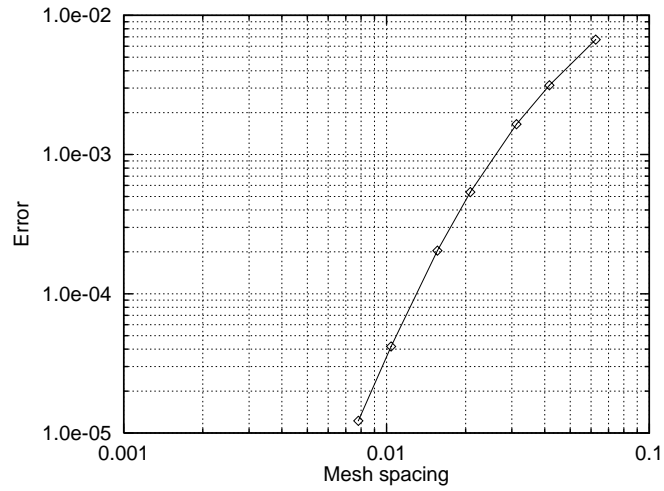


FIG. 3.8. Numerical error in HOC formulation exhibits 4th order dependence on mesh spacing for Problem 1 (with  $c = d = 200$ ).

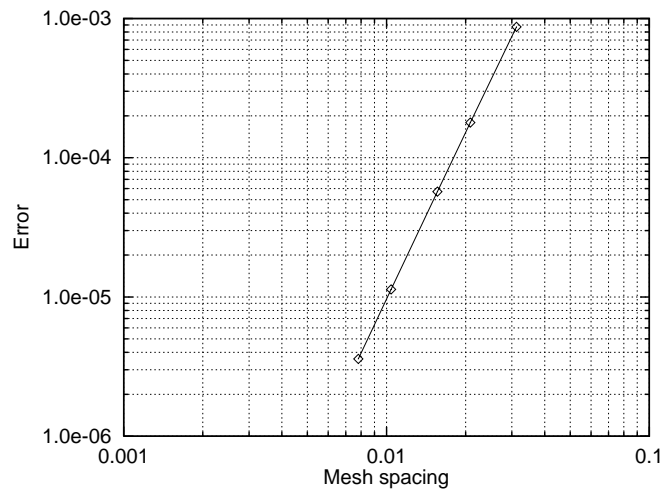


FIG. 3.9. Numerical error in HOC scheme for Problem 2 with  $c = d = 200$  also demonstrates 4th order behavior.

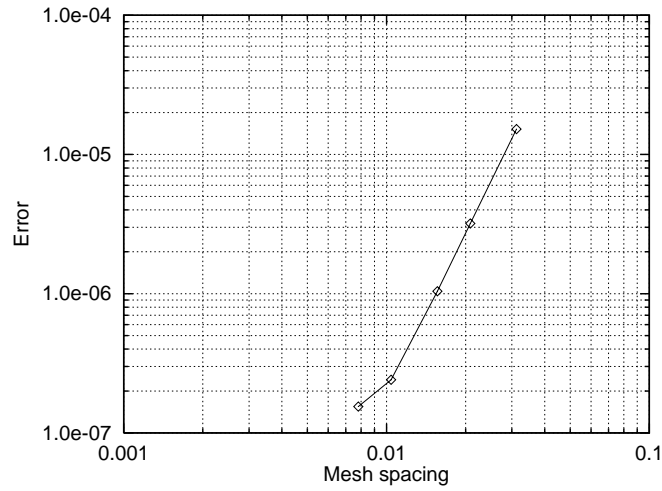


FIG. 3.10. Numerical error in HOC scheme for Problem 3 with  $R = 200$  demonstrates 4th order behavior.

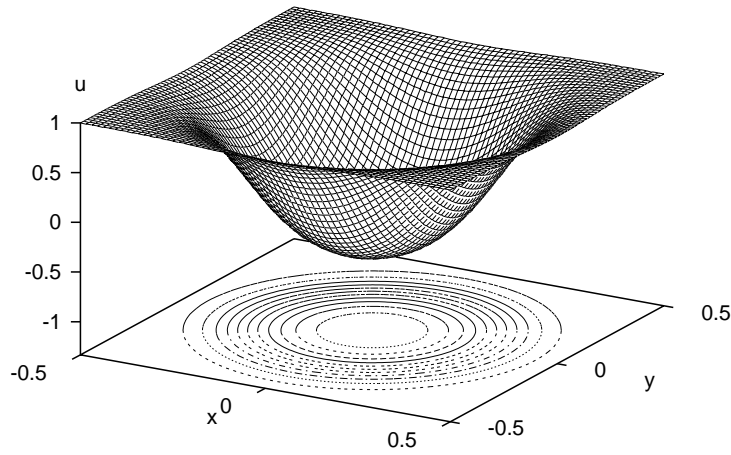


FIG. 3.11. Surface plot of numerical solution for Problem 2 with  $c = d = 500$  using the same fine grid and multigrid cycle as in Fig. 3.2.

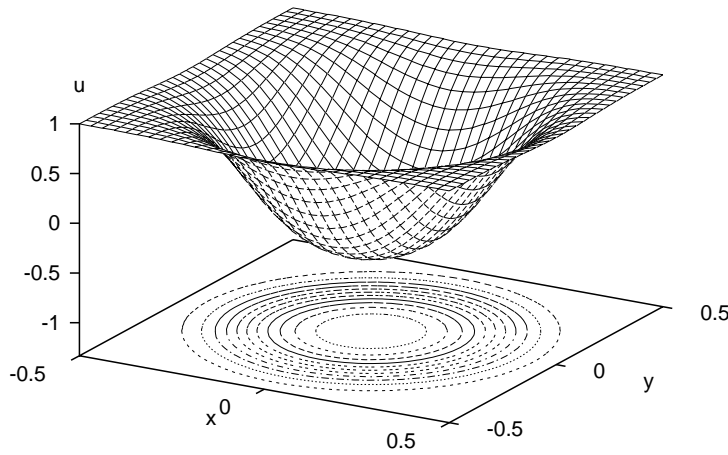


FIG. 3.12. Numerical solution for Problem 2 with  $33 \times 33$  fine grid and  $c = d = 200$  as in Fig. 3.6.

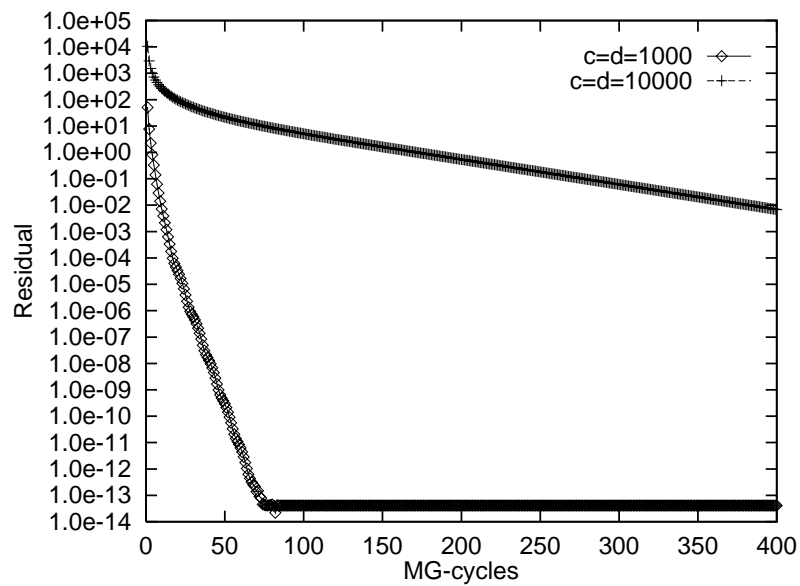


FIG. 3.13. Residual versus multigrid cycles for Problem 1 with large  $c, d$  using the same grid and cycling strategy as Fig. 3.1.